STUDY OF PRESTRESS TRANSFER THROUGH BEARING ANCHORAGE AND TRANSFER BOND OF PRETENSIONED HOLLOW PRESTRESSING BAR

(Translation from Proceedings of JSCE, No.679/VI-51, Jun 2001)



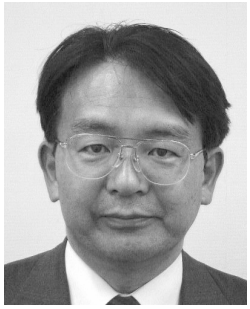


Masafumi IMAI Takashi IDEMITSU Tsutomu YOKOTA Shigeru MIZOGUTHI

The use of a prestressing bar manufactured in the shape of pipe makes it possible to induce prestress into concrete for pretensioning without the need for end anchorages (abutments) at which to tension and anchor the tendon. Known here as the HPC system, this results in a complex with the concrete member consisting of transfer bonding along the pipe thread and bearing anchorage arising from the nut used for anchorage. In a this study, the characteristics of transfer bonding along the thread and the bearing anchorage are separately investigated and this complex anchorage is quantified through experiments. Consequently, it is confirmed that complex anchorage behavior is exhibited by both transfer bonding and the bearing anchorage. Furthermore, it is confirmed through a full-scale experiment that the HPC system offers adequate performances in teams of anchorage strength and time-dependent properties.

Keywords: *prestressed concrete, pretensioning system, transfer bonding, bond stress, slip*

Masafumi IMAI is a engineer of Research Laboratory of Oriental Construction Co., LTD. He is a member of JSCE.

Takashi IDEMITSU is a Professor in the Department of civil engineering at Kyushu Institute of Technology, Japan. He is a member of JSCE.

Tsutomu YOKOTA is a engineer of Technical Division of Oriental Construction Co., LTD.

Shigeru MIZOGUTHI is a engineer of Engineering Section, Specialty Steel & Wire Products Division of Neturen Co., LTD.

1. INTRODUCTION

Pretensioning normally requires large stiff end-anchorages (referred to here as abutment) to which the tensioned tendons are anchored. This study aims at achieving pretensioning without the need for abutment by using prestressing bars that are manufactured as pipes with high tensile strength. The pipes are referred to as "Hollow Prestressing Bars" (HPBs), and an anchorage system using these HPBs is called an HPC system.

The system is schematically described in **Figure 1**. Prestressed concrete members are produced with this system using the following procedure.

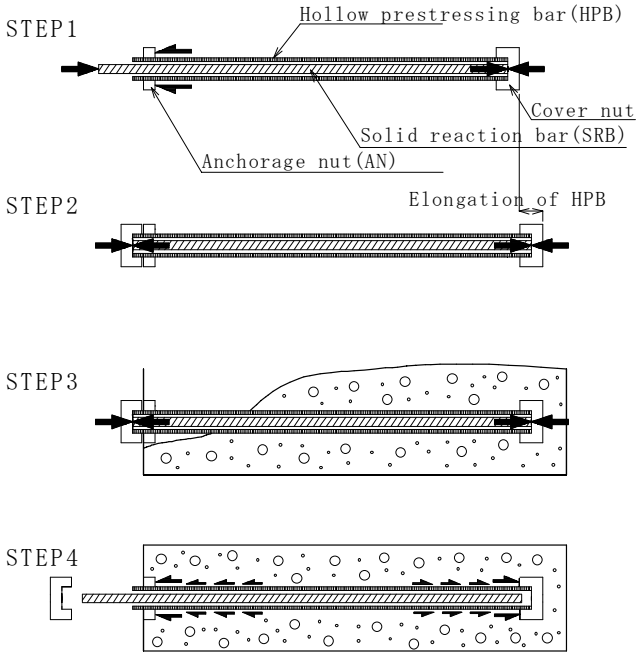

Fig.1 Manufacture of prestressed concrete member using HPC system

STEP 1: A solid reaction bar (SRB) is inserted into the HPB, which is closed with a cover nut at the other end. The HPB is tensioned with a jack by exerting a reaction on the SRB. The prestressing force is transferred to the HPB through the anchorage nut (AN).

STEP 2: Once the required prestressing force (tension) has been induced in the HPB, the HPB is anchored using a second cover nut. The tension in the HPB and the compression in the SRB are then balanced, providing an independent pretensiond HPB.

STEP3: The pretensioned HPB is placed in its final position in the formwork and the concrete is cast.

STEP4: Once the concrete has hardened sufficiently, the cover nut at the end where the tensioning was applied is removed and the prestressing force is transferred to the concrete through both the bearing anchorage and the transfer bond between the concrete and the thread cut at the end of the HPB[1].

Thus, the HPC system makes it possible to construct pretensioned concrete members anywhere without the limitations imposed by the need for abutments.

The HPC system as a pretensioning method is characterized by (1) no expensive anchorage devices, (2) no grout injection, and (3) no tensioning equipment such as jacks and pumps, because the only site work required is release of the cover nut, tensioning is precisely controlled because it can be done in a well-equipped factory.

Practical implementation of the HPC system will make it possible to reduce construction site labor requirement while also extending the application of prestressed concrete into fields such as repair and strengthening, where such technology concrete has not so far been employed.

2. MECHANISM OF THE COMPLEX ANCHORAGE

(1) Outline of mechanism of the complex anchorage

Figures 2 (a) and (b) show schematically the mechanism of the complex anchorage of the HPB before and after prestressing, respectively. **Figures 2** (c), (d), and (e) describe the relationships between distance x from the rear surface of the AN and tension $P(x)$ in the HPB, bond stress $\tau(x)$, and slip $S(x)$, respectively. We refer to the tensioning end as the member end and the rear surface of the AN as the anchorage end. Boundary conditions for study of the anchorage mechanism are as follows:

a) If it is assumed that prestressing force is contributed by the bearing anchorage due to the AN and transfer bonding along the thread, we obtain Eq.(1).

$$P_t = P_n + P_b \tag{1}$$

where P_t : prestressing force (tension) induced in the HPB
P_n : bearing force contributed by the AN bearing anchorage
P_b : bonding force contributed by transfer bonding along the thread

b) The slip ($S(0)$) between the HPB at the anchorage end and concrete due to prestressing must equal the deformation (contraction) (δ) of the AN, because the AN is stiffly fixed to the HPB by the thread at the member end.

$$\delta = S(0) \tag{2}$$

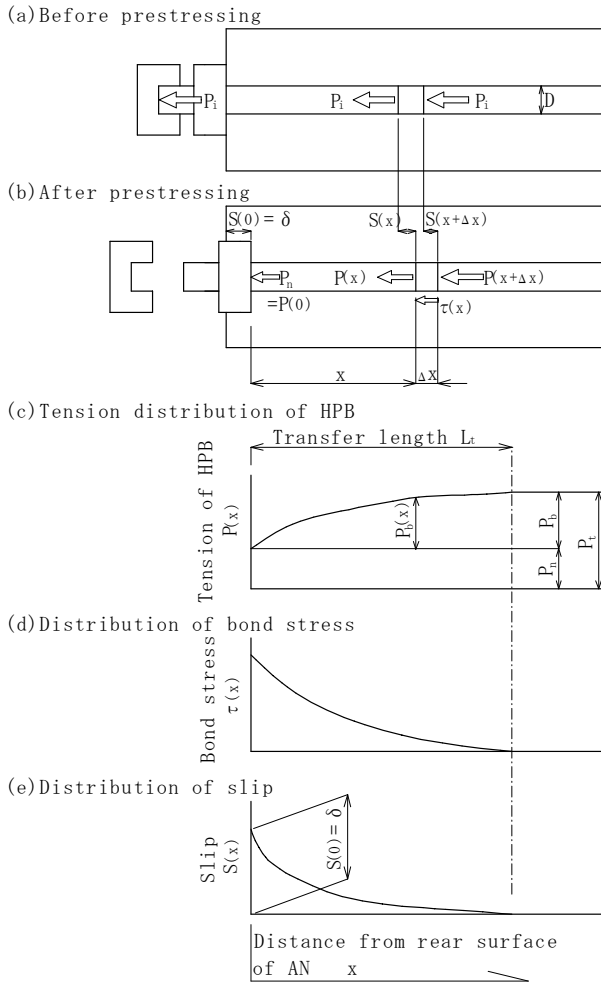

Fig.2 Schematic of mechanism of complex anchorage

Therefore P_n, P_b, and $P_b(x)$ can be obtained under the boundary conditions mentioned above using the relationship between $P_b(x)$ and $S(x)$, which is dependent on the bond characteristics of the thread, and the relationship between P_n, which acts on the AN, and δ.

(2) Outline of stress analysis in the anchorage zone

If the tension $P(x)$ in the HPB at distance x from the anchorage end is available, the tension in the HPB at distance $x + \Delta x$ can be obtained using Eq.(3).

$$P(x + \Delta x) = P(x) + \tau(x) \cdot \pi \cdot D \cdot \Delta x \tag{3}$$

where D: diameter of the HPB

Generally, slip is considered as a relative slip between the concrete and steel. However, slip is defined here as the deformation of the HPB at each point with respect to a located at the transfer length from the anchorage end, where no slip takes place (referred to below as the transfer end). In this definition, the slip $S(x)$ at distance x from the anchorage end can be expressed items of contraction of the HPB:

$$S(x) = \sum_{n=1}^{(L_t - x)/\Delta x} \frac{P_t - P(x + n \cdot \Delta x)}{A_p \cdot E_p} \cdot \Delta x \tag{4}$$

where L_t : transfer length
A_p : area of the HPB
E_p : Young's modulus of the HPB

If the slip $S(x)$ at distance x from the anchorage end is known, slip $S(x+\Delta x)$ can be obtained in Eq.(5).

$$S(x+\Delta x) = S(x) - \frac{P_t - P(x+\Delta x)}{A_p \cdot E_p} \cdot \Delta x \tag{5}$$

The relationship between bond stress $\tau(x)$ and slip $S(x)$ is experimentally obtain in Eq.(6)[6].

$$\tau(x) = f_1\big(S(x)\big) \tag{6}$$

$$P_n = f_2(\delta) \tag{7}$$

If it is assumed that the relationship between bearing force P_n contributed the AN and deformation (δ) of the AN is given by Eq.(7), the relationships between $P(x)$, $\tau(x)$, and x, which are shown in **Figures 2**(c), (d), and (e), can be obtained by the following procedure:

a) select Δx
b) assume δ to be $S(0)$
c) calculate P_n using Eq.(7). $P_n = P(0)$
d) substitute $S(0)$ into Eq.(6) to get $\tau(0)$
e) $x = 0$
f) compute $P(x+\Delta x)$ using Eq.(3)
g) calculate $S(x+\Delta x)$ using Eq.(5)
h) get $\tau(x+\Delta x)$ using Eq.(6)
i) repeat steps f) through h) for $x = \Delta x$, $x = 2\Delta x$, $x = 3\Delta x$, , , , , , , ,
j) if $P(x+\Delta x)$ dose not equate to P_t when $S(x+\Delta x) = 0$, assume the choice of $S(0)$ is not appropriate. Repeat until $P(x+\Delta x) = P_t$, assuming $S(0) = \delta$.
k) when $P(x+\Delta x) = P_t$ at $S(x+\Delta x) = 0$ is obtained, iteration is complete and transfer length $x+\Delta x$ is obtained. The distributions of $P(x)$, $\tau(x)$, and $S(x)$ represent the relationships between tension in the HPB $P(x)$, bond stress $\tau(x)$, and slip $S(x)$ and distance x from the anchorage end.

3. OUTLINE OF BASIC EXPERIMENTS

The mechanism of the HPC complex anchorage is described in section 2. The contributions made by bonding force (P_b) as a result of transfer bonding along the thread and the bearing force (P_n) resulting from the AN bearing anchorage to total prestressing force (P_t) depend on the respective characteristics of transfer bonding along the thread and the AN. Transfer bonding characteristics are described by relationship between bond stress and slip in Eq.(6) $(\tau - S)$, while the anchorage characteristics are given by the relationship between bearing force and deformation of the AN in Eq.(7) $(P_n - \delta)$. Pretensioned Specimens bearing area of the AN and cross-section concrete area as parameters are used to verify the complex anchorage mechanism as described in section 2. Through these experiments, the ratio of contributions made by the bearing anchorage and transfer bonding, as well as the anchorage characteristics of the AN $(P_n - \delta)$ and the bonding characteristics of the thread $(\tau - S)$, are investigated.

(1) Characteristics of the HPB

Table-1 shown the characteristics of the HPB used in these experiments. They are designed to be the same as those of conventional prestressing bars. **Figure 3** shows the shape of the thread, which is also the same as that of conventional prestressing bars of the same diameter.

(2) Dimensions of specimens and parameters investigated

Table-1 Mechanical properties of HPB

Outer diameter (mm)	Inner diameter (mm)	Cross-sectional area (mm^2)	Nominal yield strength (N/mm^2)	Nominal tensile strength (N/mm^2)	Young's modulus (kN/mm^2)
32	22	424.1	930	1080	196

Pretensioned specimens are produced in the conventional manner by using abutments, with an initial prestressing force of the HPB (P_i) is 294kN (σ_{pi} = 693 N/mm^2). The HPC system is not suitable for pretensioning in these experiments, because the strain gages required on the inner surface of the HPB wand prevent the SRB being threaded through the HPB. However since here is no difference in the tensioned tendons between the two systems aside from the reaction mechanism, it is considered that there is no difference in anchorage properties.

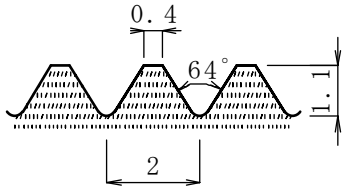

Fig.3 Shape of thread cut at end of HPB (Unit: mm)

A general view of specimens is shown in **Figure 4**. **Table-2** summarizes the dimensions and parameters considered.

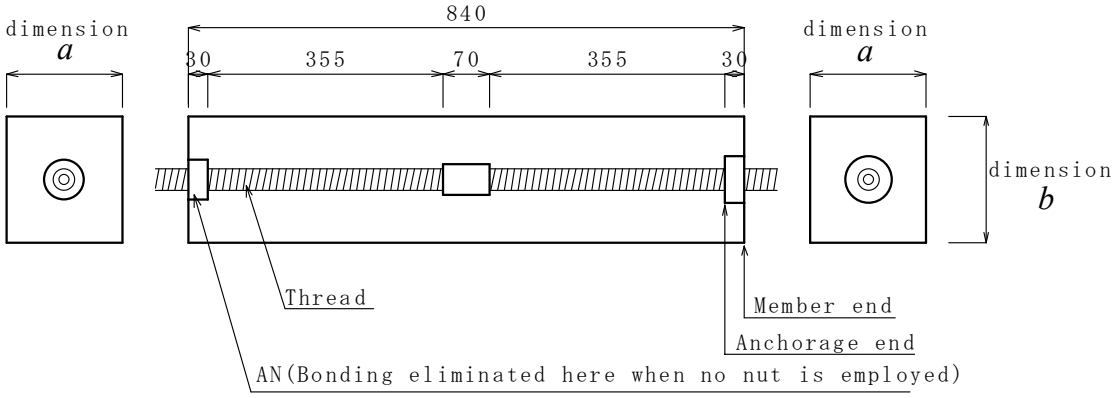

Fig.4 General view of the specimen (Unit: mm)

Table-2 Dimensions of specimens and parameters considered

Specimen designator	Properties of concrete		Dimensions of specimen			AN		Ratio of bearing area to concrete area
	Compressive strength f'_c (N/mm^2)	Young's modulus E_c (kN/mm^2)	dimension a (mm)	dimension b (mm)	Area *1 A_c (mm^2)	Diameter ϕ (mm)	Area *1 A_n (mm^2)	A_n / A_c (%)
M0	30.4	26.5	175	190	32395	0	0	0.00
Ms						50	1108	3.42
Mm						60	1972	6.09
Mb						70	2993	9.24
B0			205	220	44245	0	0	0.00
Bs						50	1108	2.50
Bm						60	1972	4.46
Bb						70	2993	6.76

*1 : Area of HPB is deducted, assuming diameter of 33mm

Letters M and B in the specimen designators indicate differences in cross-sectional area parameter. M means that the sectional dimension a is 175mm, a value determined taking into account the

minimum depth of the member in anchorage system 1S19.3, in which SWPR19-19.3 is used, because the HPB used has almost the same characteristics as this 19-wire-strand 19.3mm cable (SWPR19-19.3mm)[7]. In B specimens sectional dimension a is increased by 30mm to 205mm. Sectional dimension b is increased by 15mm in line with dimension a in order to ensure that cracks develop in the narrower surface.

Similarly, 0, s, m, and b in specimen designators indicate the bearing area of the AN. 0 represents the case without a nut, m for a nut of standard bearing area for a prestressing bar of ϕ32mm, s for half m, and b for 1.5 times m.

As shown in **Figure 4**, the whole length of the HPB is cut with a thread. The AN is fixed to the end of the HPB by turning it onto the thread. In the case of specimens without the AN, bonding is eliminated over the length that would otherwise be taken up by the AN to keep the transfer length constant.

Specimens have different anchorage conditions. The HPB includes a joint at the center, because the length of the HPB is limited by the need to glue strain gages to the inner surface of the HPB.

(3) Position of strain gages

Figure 5 shows the position of strain gages. Gages are glued to the inner surface of the HPB so as to presence bonding along the thread. Two gages are attached to opposite sides of the HPB pipe at each position so as to eliminate any influence of bending.

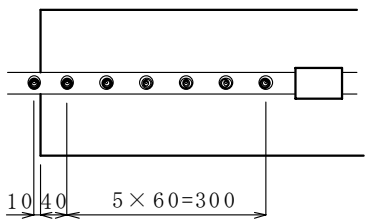

Fig.5 Position of strain gages (Unit: mm)

(4) Calculating tension in the HPB, bond stress, and slip

a) Strain distribution along the tendon
Assuming that the strain distribution can be approximated by a parabolic curve, parabolic curves are regressed from experimental results taken at three adjacent points [7].

b) Tension in the HPB
The tension in the HPB is taken to be the steel strain. The relationship between HPB tension and strain is calibrated in advance, because the area of the threaded length of the HPB is different from the nominal cross-sectional area of the tendon.

c) Bond stress
Bond stress along the tendon at any position is obtained from the tendon's strain distribution. It can be calculated with Eq.(8) using the gradient of the strain distribution curve.

$$\tau = \frac{A_p \cdot E_p}{\pi \cdot D} \cdot \frac{d\varepsilon}{dx} = \frac{k}{\pi \cdot D} \cdot \frac{d\varepsilon}{dx} \tag{8}$$

where τ : bond stress
A_p : area of tendon
E_p : Young's modulus of tendon
D : diameter of tendon
$\frac{d\varepsilon}{dx}$: gradient of strain distribution at arbitrary position
k : coefficient obtained through calibration (refer to 3.(4).b))

d) Slip
As mentioned before, slip is defined in this investigation as the deformation of the HPB at each point with respect to the transfer end [7]. The slip at any point is calculated by integrating the difference in strain between the required prestressing force (constant) and HPB tension from the transfer end to the that point.

4. RESULTS OF BASIC EXPERIMENTS AND DISCUSSION

Figure 6 (a) and (b) show the tension distribution in the HPB for M and B specimens, respectively. Here, dots represent tension in the HPB as computed from the measured strain, while the curves are converted from the strain distribution curve, which is calculated as described in section 3.(4). "CAL" is the computed prestressing force as obtained from the initial prestressing force. **Figure 6** demonstrates that HPB tension coincides with the induced prestressing force at any distance from the anchorage. This in turn clarifies that tendons are well anchored in an specimens with varying parameters of cross-sectional area and AN bearing area. Observing the tension distribution of the HPB over the Whole anchorage zone (from the anchorage end to the transfer end), it is clear that the test parameters have a significant influence on the results.

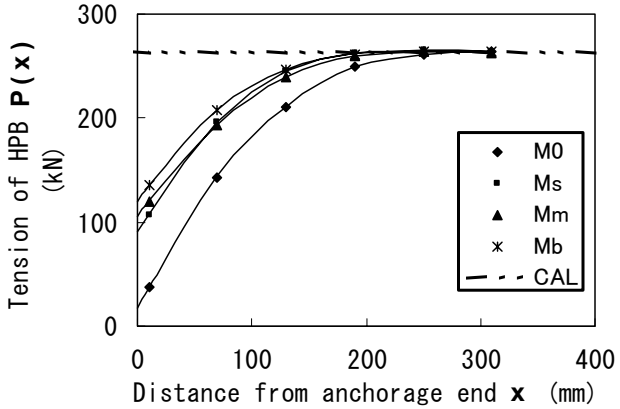

(a) Specimen M

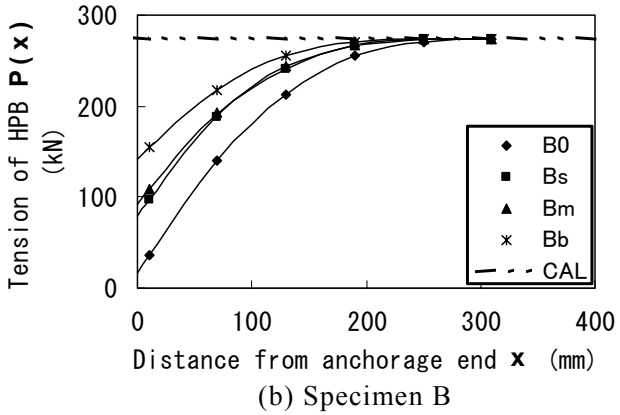

(b) Specimen B

Fig.6 Tension distribution of HPB

Table-3 shows ratio of AN bearing area (A_n) to the cross-sectional area of concrete (A_c) (A_n / A_c; the bearing area ratio); the prestressing force (P_t); the bearing force contributed by the AN (P_n); the bonding force contributed transfer bonding along the thread (P_b); the ratio of bearing force to prestressing force (P_n / P_t ; the bearing contribution ratio); and the transfer length (L_t), which is the length from the anchorage end to the point where the tension in the HPB reaches 95% of the prestressing force.

Table 3 Summary of bearing force contributed by bearing anchorage and bonding force contributed by transfer bonding

Specimen designator	Ratio of bearing area to concrete area A_n / A_c	Required prestressing force P_t (kN)	Bearing force P_n (kN)	Bonding force P_b (kN)	Ratio of bearing force to prestressing force P_n / P_t	Transfer length at 0.95 L_t (mm)
M0	0.0000	263.3	0.0	263.3	0.000	194
Ms	0.0342	264.4	90.2	174.2	0.341	140
Mm	0.0608	262.8	106.0	156.8	0.403	155
Mb	0.0922	264.1	120.2	143.9	0.455	138
B0	0.0000	273.3	0.0	273.3	0.000	204
Bs	0.0250	273.5	78.5	195.0	0.287	169
Bm	0.0445	273.6	92.0	181.6	0.336	166
Bb	0.0676	273.5	142.2	131.3	0.520	141

The bearing force contributed by the AN bearing anchorage end, while the bonding force contributed by the transfer bonding along the thread is assumed to be the remainder of the bearing force. The characteristics of transfer bonding along the thread and the AN bearing anchorage are discussed in the following sections as a verification of the mechanism described in Section 2.

(1) Characteristics of AN bearing anchorage

As described in Section 2, the aim is to express the characteristics of the AN bearing anchorage in the form of the relationship between bearing force and deformation of the AN ($P_n - \delta$). Since the AN is fixed to the HPB through the thread, the deformation of the AN (δ) must be the slip of the HPB at the anchorage end.

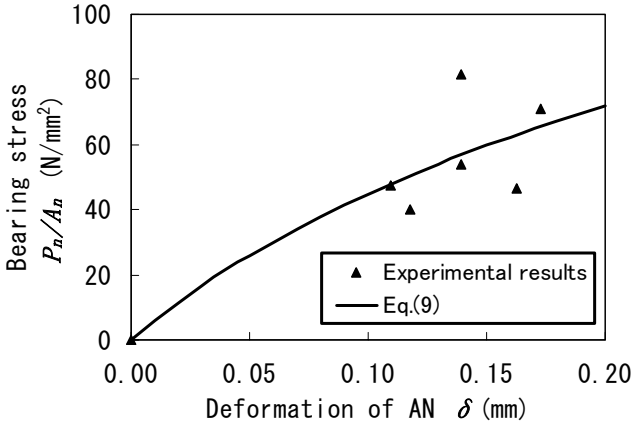

Fig.7 Relationship between bearing stress and deformation of the AN

Figure 7 shows the relationship between AN deformation and bearing stress, as obtain dividing the bearing force by the bearing area of the AN. From this Figure, it can be said that there is a loose correlation between bearing stress and AN deformation. The regression is expressed in Eq.(9). The square of the correlation coefficient, r, which shows a scatter, is $r^2 = 0.746$.

$$\frac{P_n}{A_n} = 70.2 \cdot \ln(1 + 8.94 \cdot \delta) \tag{9}$$

Eq.(9) represents the same relationship as giving by Eq.(7) in Section 2. However, Eq.(9) has a large scatter, partly because it is derived from a very loose correlation that could be a consequence of the small number of specimens.

Additionally the influences of concrete properties such as elastic deformation, which affect δ, are not taken into account because the same concrete is used for all specimens. Future investigations should look at the influence of concrete properties so as to gain a more reliable relationship between P_n and δ.

From **Figure 7**, the bearing stresses are 40-80N/mm^2, which corresponds to 1.3-2.6 times the concrete compressive strength. For safety, the bearing stress should be within one third of the concrete strength [9]. Not only the bearing stress but also the bearing strength of the concrete must be considered in the anchorage zone of the HPC system [10].

(2) Bond characteristics along the thread

Figure 8 shows the relationship between bond stress and slip, obtained as described in Section 3.(4). Numerical integration is carried out from 0 (the anchorage end) to 310mm in 30mm steps to calculate bond stress and slip at this distance from the anchorage end. The regression is expressed by Eq.(10), which is shown in **Figure 8** as a solid line. The square of the correlation coefficient, r, which shows a scatter, is $r^2 = 0.975$.

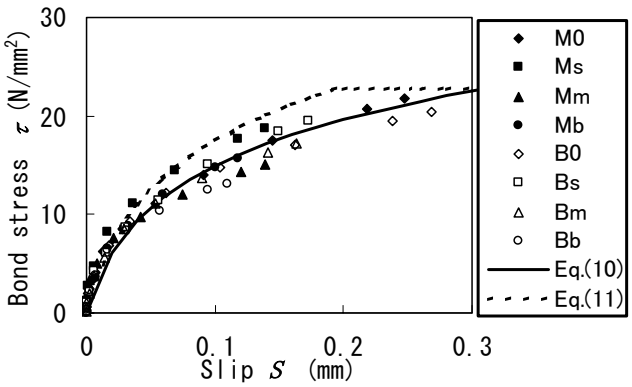

Fig.8 Relationship between bond and slip

$$\tau = 7.55 \cdot \ln\left(1 + 2000 \cdot \frac{S}{D}\right) \tag{10}$$

$$\tau = 1.6 \cdot \sqrt{f'_c} \cdot \ln\left(1 + 2000 \cdot \frac{S}{D}\right) \quad (11)$$

where S : slip (mm)
D : diameter of tendon (mm)
f'_c : compressive strength of concrete (N/mm^2)

As shown in **Figure 8**, the $\tau - S$ relationship in the region of the thread has almost no dependence on the test parameters, cross-sectional area of concrete and AN bearing area. Consequently, the $\tau - S$ relationship can be closely regressed by an equation. It can be said that the bond characteristics of the thread are not affected by the cross-sectional area of concrete, the existence of the AN, and the bearing area of the AN. In **Figure 8**, the $\tau - S$ relationship, which is obtain in a pull-out test and regressed in Eq.(11), is also shown by the dotted line. The bond stress computed in Eq.(10) is slightly smaller than that of Eq.(11). The deviation could be within experimental and regression errors. Further investigation of this issue is required.

If bearing force P_n is known, substituting the $\tau - S$ relationship computed using Eq.(10) into Eq.(6) as given in Section 2 yields the tension distribution of the HPB, the bond stress distribution, and the slip distribution through iteration. In carrying out this iteration, Δx is taken to be 2mm and the experimental results for P_t and P_n are used.

Figures 9, **10**, and **11** give examples of the numerical and experimental results of tension distribution in the HPB, bond stress distribution, and the slip distribution, respectively. As these Figures clearly show, the numerical and experimental results agree well. Therefore, it is confirmed that if the bearing force contribution P_n to prestressing force P_t is known, the distributions of tension in the HPB, bond stress, and slip are available. These numerically and experimentally obtained distributions are similar to those shown in Figure.2 (c), (d), and (e).

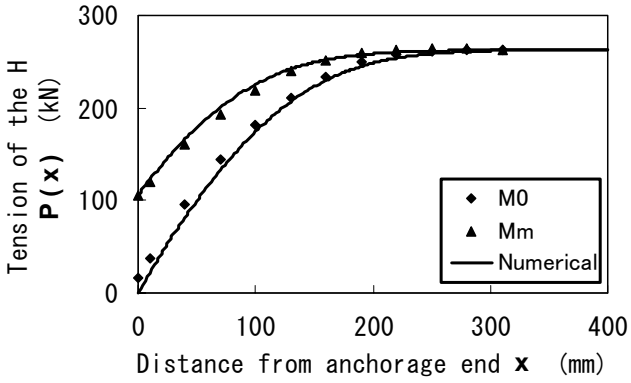

Fig.9 Distribution of tension in the HPB

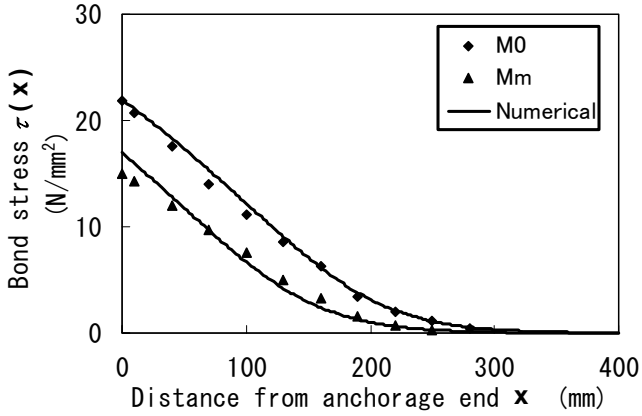

Fig.10 Distribution of bond stress

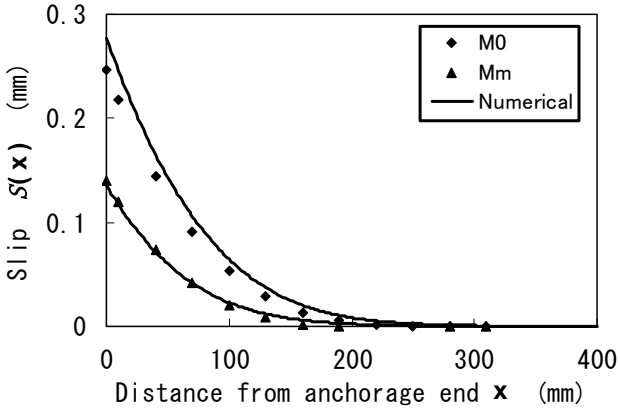

Fig.11 Distribution of slip

(3) Verification of complex anchorage mechanism

Section 2 describes how to quantify complex the anchorage in terms of tension distribution in the HPB, transfer length, etc, using the bond characteristics, which are expressed by relationship between bond stress and slip (Eq.(6)). Also described are the anchorage characteristics of the AN, which are exhibited in the relationship between force acting on the AN and deformation of the AN (Eq.(7)).

Table-4 Comparison between numerical and experimental results

Specimen designator	Bearing force P_n (kN)			Bonding force P_b (kN)			Transfer length L_t (mm)		
	Experimental	Numerical	N/E	Experimental	Numerical	N/E	Experimental	Numerical	N/E
M0	0.0	0.0	1.00	263.3	263.3	1.00	194	208	1.07
Ms	90.2	73.6	0.82	174.2	190.8	1.10	140	172	1.23
Mm	106.0	108.1	1.02	156.8	154.7	0.99	155	152	0.98
Mb	120.2	136.6	1.14	143.9	127.5	0.89	138	134	0.97
B0	0.0	0.0	1.00	273.3	273.3	1.00	204	210	1.03
Bs	78.5	75.9	0.97	195.0	197.6	1.01	169	174	1.03
Bm	92.0	112.3	1.22	181.6	161.3	0.89	166	154	0.93
Bb	142.2	141.3	0.99	131.3	132.2	1.01	141	136	0.96

Eq.(10) is substituted into Eq.(6) and Eq.(9) into Eq.(7) to determine the contributions made by bearing anchorage and transfer bonding, as well as the transfer length. Numerical and experimental results are tabulated in **Table-4**.

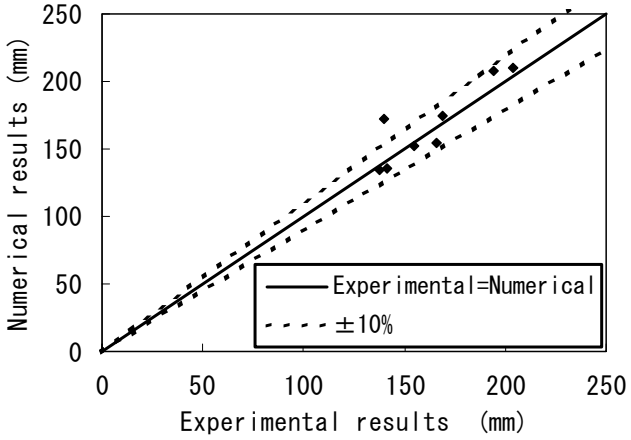

Fig.12 Comparison of transfer length between numerical and experimental results

Figure 12 compares the transfer length as obtained in the experimental and numerical results. The solid line in this Figure represents the coincidence between the results and the dotted line indicate boundary ratios of experimental results to numerical results, one for a ratio of 0.9 and the other for 1.1. The transfer length is the length from the anchorage end to the position where the tension in the HPB coincides with the required prestressing force. Since, as shown in **Figure 9**, the tension in the HPB gradually approaches the prestressing force near the transfer end, it is not easy to define the transfer length precisely. Therefore in this paper the transfer length is define as the length from the anchorage end to the position where the tension in the HPB reaches 95% of the prestressing force (P_t)[2]. As shown in **Figure 12**, the experimental and numerical results agree to within ±10%. From **Table-4**, the bearing force and bonding force are simulated within ±20% and ±10%, respectively.

This investigation confirms that the complex anchorage of the HPC system can be quantified in accordance with the mechanism as discussed in Section 2. However, the bond characteristics of the thread (Eq.(10)) and the bearing characteristics of the AN (Eq.(9)) have been determined from limited experimental results. These characteristics should be investigated further, particularly with respect to the properties of concrete.

5. EXPERIMENTS ON EXISTING STRUCTURE TO CONFIRM ANCHORING PERFORMANCE OF THE HPC SYSTEM

In strengthening a concrete girder with external tendons, an anchorage block has to be positioned so as to anchor the tendons. In this Section, an experiment is performed on an existing bridge by fixing concrete anchorage blocks stiffly to the existing concrete girder using the HPC system, is described.

Figure 13 describes the system schematically. In this type of work, concrete anchorage blocks are normally attached by post-tensioning, making it very difficult to control the prestressing precisely. This is the elongation of a short tendon during prestressing is very small. Furthermore, heavy prestressing equipment such as jacks place on enormous burden on laborers working in the

confined space under and between existing girders.

Applying the HPC system in this situation makes it possible to; (1) introduce an exact prestress without controlling prestressing on site; (2) avoid grout injection; and (3) save labor costs because only a light electric torque wrench is required to release the tensile force of the HPB on site.

The aim of this experiment is to confirm the anchoring performance of the HPC system in a practical structure [8], and observations of tension in the HPB are continued for half a year. Details of HPB placement are in **Figure 14**.

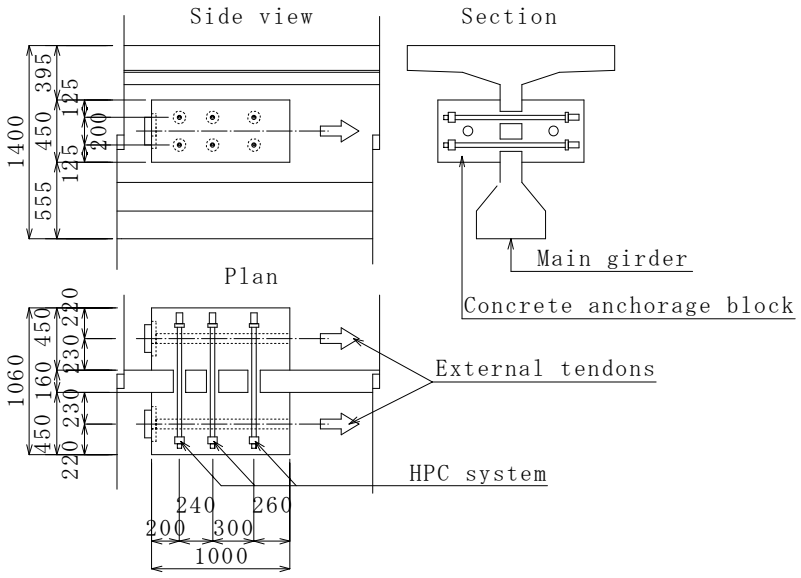

Fig.13 Schematic description of system (Unit: mm)

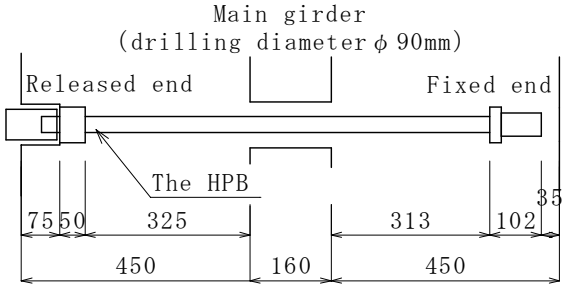

Fig.14 Detail of HPB (Unit: mm)

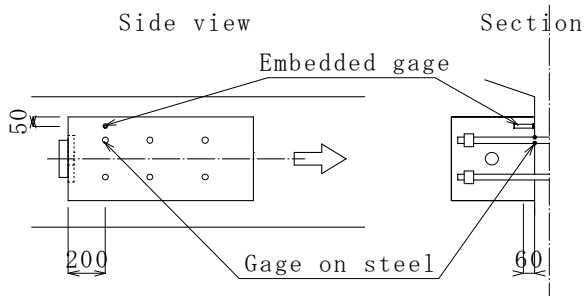

Fig.15 Position of gages (Unit: mm)

The transfer length of the HPC system is here confirmed and the conditions are as follows;
a) Initial prestressing force: P_i = 294kN
b) Bearing area of AN: A_n = 1,972 mm^2
c) Cross-sectional area of concrete: A_c = 49,770 mm^2
(225 × 225mm is assumed; the area of the tendon is subtracted from the 225 × 225mm cross-section.)
d) Area of HPB: A_p = 424.1 mm^2
e) Compressive strength of concrete: f'_c = 55.3 N/mm^2
f) Young's modulus of concrete: E_c = 31,300 N/mm^2
g) Young's modulus of HPB: E_p = 196,000 N/mm^2

The prestressing force in the HPB is reduced due to elastic shortening of the concrete from P_i to P_t. The calculated prestressing force (P_t) of the HPB at the position of the gages shown in **Figure 15** is 283kN.

The bond characteristics of the thread are determined according to the method described in Section 2 using Eq.(11) and Eq.(9). This shows that the prestressing force P_t of 283kN is made up of a bearing force P_n of 99kN and a bonding force P_b of 185kN.

The tension distribution in the HPB is shown in **Figure 16**. Distance $L_{0.95P_t}$ from the anchorage end to the position at which the tension in the HPB is 95% of the required prestressing force is

122mm (indicated as transfer length for $0.95P_t$ in the figure) and distance $L_{0.99P_t}$ from the anchorage end to the position at which the tension in the HPB is 99% of the prestressing force is 178mm (indicated as transfer length for $0.99P_t$ in the figure).

As is clear in **Figure 14**, the distance from the rear surface of the AN to the interface between the concrete anchorage block and the existing girder is 312mm and 325mm on the two sides, respectively, which is greater than this transfer length.

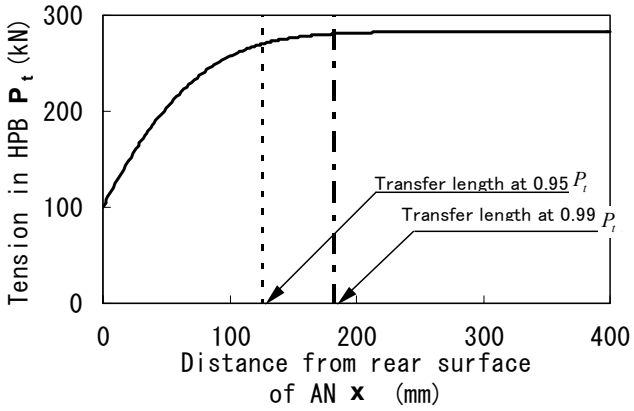

Fig.16 Distribution of tension in HPB

The bearing stress due to the bearing force contributed by the AN anchorage is 50.2N/mm^2. Eq.(12) is derived from bearing test using the AN to predict bearing strength of concrete [10].

$$f'_{ak} = 5.18 \cdot \sqrt{f'_c} \cdot K \cdot \sqrt{\frac{A_c}{A_n}} \tag{12}$$

where f'_{ak}: bearing strength (N/mm^2)
f'_c : compressive strength of concrete (N/mm^2)
A_n : bearing area of AN (mm^2)
A_c : cross-sectional area of concrete (mm^2)
K : constant depending on re-bar quantity $= 0.531 \cdot t + 0.897$
t : equivalent thickness with re-bars assumed to be cylinders

When there are no re-bars, the bearing strength from Eq.(12) is 173.6N/mm^2,which corresponds to 3.1 times the concrete compressive strength and to three times the bearing stress of 50.2N/mm^2, providing a safety factor of three.

Table-5 tabulates changes in steel and concrete strains measured at the points shown in **Figure 15**. Strains are measured in four anchorage blocks designated No.1 through No.4. The calculated value given in the table is that of strain converted from the prestress loss due to elastic shortening. As **Table-5** shows changes in concrete strains are approximately 1.3 times the calculated value. This means that more prestress is induced than required at the gage positions. This is partly because the distribution of prestress is not uniform in the anchorage zone, where the gages are located.

Table-5 Change in concrete and steel strains ($\times 10^{-6}$)

	Concrete	HPB	Numerical
No.1	−151	−188	−135
No.2	−166	−203	
No.3	−189	−206	
No.4	−172	−176	

"−" indicates contraction.

Figure 17 shows the time-dependent changes in concrete strain in No.2 block. The time-dependent change in HPB prestressing force is shown in **Figure 18**; here prestressing force is converted from the measured steel strain of the HPB. The numerical results of concrete strain shown in **Figure 17** are computed as bellows. Numerical results in **Figure 18** are converted from the numerical time-dependent changes in concrete strain.

Until prestressing of external tendons,

$$\varepsilon_{ct} = \varepsilon_{cp} \cdot (1 + \phi_{pt}) + \varepsilon_{sht} \tag{13}$$

After prestressing of external tendons,

$$\varepsilon_{ct} = \varepsilon_{cp} \cdot (1 + \phi_{pt}) + \varepsilon_{cl} \cdot (1 + \phi_{lt}) + \varepsilon_{sht} \tag{14}$$

where ε_{ct} : concrete strain at age t
ε_{cp} : elastic strain of concrete at HPB prestressing (measured value)
ε_{cl} : elastic strain of concrete at prestressing of external tendons (measured value)
ϕ_{pt} : creep coefficient at time t after prestressing of the HPB [9]
ϕ_{lt} : creep coefficient at time t after prestressing of external tendons [9]
ε_{sht} : shrinkage strain from prestressing of the HPB to time t

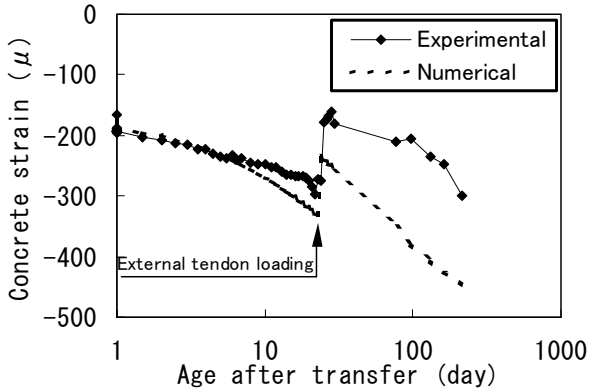

Fig.17 Time-dependent changes in concrete strain in anchorage block

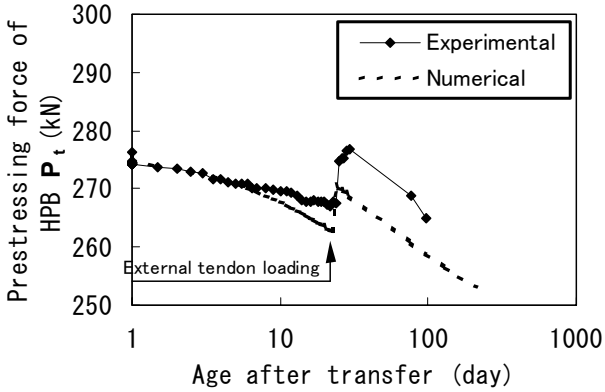

Fig.18 Time-dependent changes in prestressing force of HPB

The concrete strain at prestressing HPB is –166 μ, as shown in **Table-5**, and the prestressing force of HPB at prestressing HPB is 277kN after taking allowance for the prestress loss corresponding to a strain of 203 μ from the initial prestressing force of 294kN. As shown **Figures 17** and **18**, the time-dependent changes in both concrete strain and prestressing force are similar to the numelical results. **Figure 18** also tells us that the HPB in the HPC system is well anchored the anchorage block, because the measured prestressing force of the HPB, exceed the numerical results in **Figure 18**.

Horizontal displacement perpendicular to the bridge axis (referred to below as the perpendicular displacement) and horizontal displacement longitudinal to the bridge axis (referred to below as the longitudinal displacement) of the anchorage block are measured when prestressing the external tendons in order to confirm the behavior of the HPC anchorage block. Measurements are performed for two blocks located on either side of the girder at the points shown in **Figure 19**.

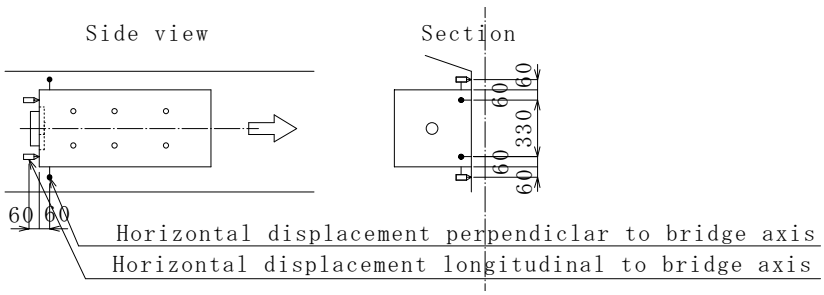

Fig.19 Position of displacement of concrete anchorage block (Unit: mm)

In **Figure 20**, the relationship between loading (prestressing force of external tendons) and perpendicular displacement is shown (this is referred to below as the $P - \delta_w$ relationship). The displacements measured at four points are averaged.

The perpendicular displacement here does not include that due to prestressing of the HPB but is that after prestressing of the external tendons. That is, since the prestress is induced at the

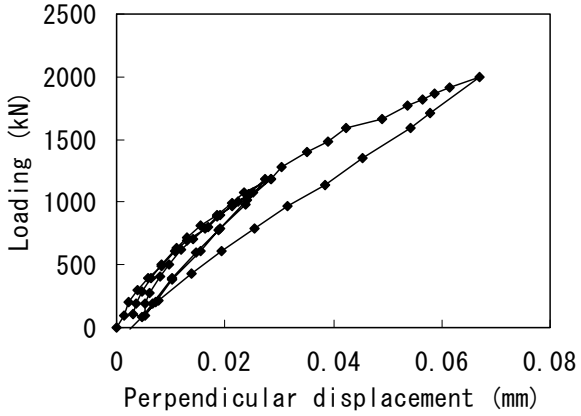

Fig.20 Relationship between loading and perpendicular displacement

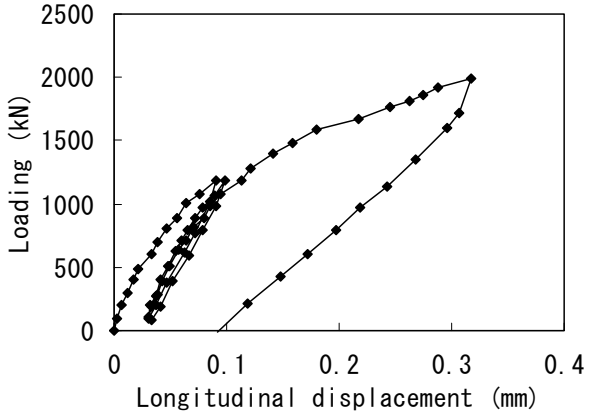

Fig.21 Relationship between loading and longitudinal displacement

interface between the girder and the anchorage block, perpendicular displacement is not necessarily the opening at the interface between the girder and the anchorage block. Loading is carried out three times up to the allowable prestressing force of external tendon at the serviceability limit state (1,176kN) and finally up to the nominal tensile strength of the external tendon (1,960kN).

As shown in **Figure 20**, the $P-\delta_w$ relationship is almost linear until the allowable prestressing force at the serviceability limit state and in the three cycles of loading the displacement returns well to the origin. Near the 1,568kN point of loading, a deflection is observed in the $P-\delta_w$ relationship. This is considered to be a decrease in rigidity due to opening of the interface of the anchorage block.

The loading at which the concrete stress at the interface between the girder and the anchorage block is visually observed near the 1,470kN loading point. This confirms, the design prestress at the interface between girder and anchorage block.

No deterioration in anchorage strength is observed in loading up to the nominal tensile strength of the tendon, 1,960kN. In de-loading, the perpendicular displacement returns to the origin.

Figure 21 shows the relationship between loading and longitudinal displacement (referred to below as the $P-\delta_d$ relationship).

As shown in the Figure, the $P-\delta_d$ relationship is almost linear, although there is some difference between the first and second loading cycles, and in cyclic loading beyond the second cycle the displacement returns well to the origin. During loading up to the nominal tensile strength of the external tendon, 1,960kN, a slight decrease in inclination of the $P-\delta_d$ curve is observed. However no deterioration in anchorage strength is apparent. The design shear transfer strength of this specimen is 2,100kN [10].

As noted above, it is confirmed that the anchorage block connected to the girder using the HPC system has satisfactory anchoring performance.

6. SUMMARY

The HPC system makes it possible to apply pretension without the need for abutments using on HPB. Conclusions regarding the HPC system as gained from the experiments described here are as follows:

(1) The complex anchorage consisting of transfer bonding along the thread and the AN bearing anchorage can be quantified in terms of the characteristics of the transfer bonding and the bearing

anchorage.

(2) The characteristics of the AN bearing anchorage are experimentally derived from the relationship between bearing stress of concrete under the AN and displacement.

(3) The characteristics of the transfer bonding of the pretensioned member are expressed by the relationship between bond stress and slip. It is confirmed that this relationship is similar to that obtained in pull-out tests.

(4) Using the characteristics of the transfer bonding along the thread, the distribution of prestressing force in HPB can be quantitatively described in anchorage zone.
(5) In strengthening a girder with external tendons, it is confirmed that concrete anchorage blocks fixed to the girder with the HPC system have satisfactory anchorage strength.

This investigation considered on HPB with an external diameter of 32mm (cross-sectional area = 424.1mm^2). Recently, new HPBs with an external diameter of 40mm (cross-sectional area = 549.8mm^2) and 43mm (cross-sectional area = 809.8mm^2) have been developed. The suitability and applicability of HPBs as determined through this research should be reconfirmed through experimental studies for HPC systems using these newly developed HPBs.

References

[1] Yokota, T., Tezuka, M., and Suzuki, M. “New Prestressing System Using Hollow Prestressing Bars”, Proceedings of FIP Symposium’93 Kyoto, Japan, Vol.1.2, pp.1087-1094, 1993
[2] Watanabe, A. “An Experimental Study on Anchorage through Bonding of Prestressing Steel used for Prestressing”, Journal of Materials, Concrete Structures and Pavements, No.25, pp.21-35, 1966 (in Japanese)
[3] Watanabe, A., Fujii, M., and Kobayashi, K. “Mechanics of Prestressed Concrete Structures”, New Series of Civil Engineering, Gihodo Publishing, pp.83-92, 1981 (in Japanese)
[4] Imai, M., Idemitsu, T., and Hashimoto, J. “Study on Transfer of Hollow Prestressing Bar used for Pretensioning Member”, Proceedings of Annual Convention of JCI, Vol.18, No.2, pp.521-526, 1996 (in Japanese)
[5] Idemitsu, T., Yamazaki, T., Watanabe, A., and Ezaki, J. “Study on Conventional Re-bars as Tendons”, Proceedings of the First Symposium on Development in Prestressed Concrete, pp.1-6, 1990 (in japanse)
[6] Imai, M., and Idemitsu, T. “Study on Bond Characteristics of Hollow Prestressing Bars”, Proceedings of Annual Convention of JCI, Vol.21, No.3, pp.361-366, 1999 (in Japanese)
[7] JSCE, “Recommendations for Prestressed Concrete Anchorage Systems (Freyssinet), Concrete Library, No.66 (in Japanese)
[8] Shima, H., Shu, R., and Okamura, H. “Bond-Slip-Strain Relationship of Deformed Bars Embedded in Massive Concrete”, Journal of Materials, Concrete Structures and Pavements, No.378/V-6, pp.165-174, 1987 (in Japanese)
[9] STANDARD SPECIFICATIONS FOR CONCRETE-1996, DESIGN, JSCE, pp.19-21, pp.215, 1996 (in Japanese)
[10] Imai, M., and Idemitsu, T. “Study on Bearing Characteristics of a Nut used at the End of a Reinforcement to Compensate Anchorage Performance”, Proceeding of Annual Convention of JCI, Vol.22, No.3, pp.1273-1277, 2000 (in Japanese)
[11] Nagai, J., Yamaguchi, K., Kitagawa, T., and Nakai, Y. “Report on Strengthening Work of SONE-Viaduct”, JOURNAL OF PRESTRESSED CONCRETE, JAPAN, Vol.37, No.6, pp.42-51, 1995 (in Japanese)
[12] STENDARD SPECIFICATION FOR CONCRETE-1996, DESIGN, JSCE, pp.26-32, 1996 (in Japanese)
[13] STANDARD SPECIFICATION FOR CONCRETE-1991, DESIGN, JSCE, pp.67-68, 1991 (in Japanese)